



**Near Constant Loss Regime in Fast Ionic Conductors  
analyzed by Impedance and NMR Spectroscopies**

Journal:	<i>Physical Chemistry Chemical Physics</i>
Manuscript ID:	CP-ART-04-2014-001773.R1
Article Type:	Paper
Date Submitted by the Author:	01-Jun-2014
Complete List of Authors:	Bucheli, Wilmer; Instituto de Ciencia de Materiales de Madrid, Arbi, Kamel; Instituto Ciencia de Materiales Madrid-CSIC, Sanz, J; Instituto Ciencia de Materiales Madrid-CSIC, Nuzhnyy, Dmitry; Institute of Physics, Academy of Sciences of the Czech Republic, Department of Dielectrics Kamba, Stanislav; Institute of Physics, Academy of Sciences of the Czech Republic, Department of Dielectrics Varez, Alejandro; Universidad Carlos III de Madrid, Materials Science Jimenez-Rioboo, Ricardo; Instituto de Ciencia de Materiales de Madrid, Materilas for the infromation technologies

Cite this: DOI: 10.1039/c0xx00000x

www.rsc.org/xxxxxx

ARTICLE TYPE

## Near Constant Loss Regime in Fast Ionic Conductors analyzed by Impedance and NMR Spectroscopies

Wilmer Bucheli<sup>a</sup>, Kamel Arbi<sup>a</sup>, Jesús Sanz<sup>a</sup>, Dmitry Nuzhnyy<sup>b</sup>, Stanislav Kamba<sup>b</sup>, Alejandro Várez<sup>c</sup> and Ricardo Jimenez<sup>a\*</sup>.

<sup>5</sup> Received (in XXX, XXX) Xth XXXXXXXXXX 20XX, Accepted Xth XXXXXXXXXX 20XX

DOI: 10.1039/b000000x

Universal dielectric response (UDR) and nearly constant loss (NCL) dispersive regimes has been investigated in fast ion conductors with perovskite and NASICON structure by using NMR and Impedance Spectroscopy (IS). In this study, electrical behavior of La<sub>0.5</sub>Li<sub>0.5</sub>TiO<sub>3</sub> (LLTO-05) perovskite and Li<sub>1.2</sub>Ti<sub>1.8</sub>Al<sub>0.2</sub>(PO<sub>4</sub>)<sub>3</sub> (LTAP0-02) NASICON compounds were investigated. In both systems a three-dimensional network of conduction paths is present. In Li-rich LLTO-05 sample, lithium and La are randomly distributed on A-sites of perovskites, but in LTAP0-02 Li and cation vacancies are preferentially disposed at M1 and M2 sites. In perovskite compound, local motions produced inside unit cells are responsible for the large “near constant loss” regime detected at low temperatures, however, in the case of NASICON compound, local motions not participating to long-range charge transport, were not detected. In both analyzed systems long-range correlated motions are responsible for dc-conductivity values of ceramic grains near 10<sup>-3</sup> S.cm<sup>-1</sup> at room temperature, indicating that low-temperature local motions, producing large NCL contribution, are not required to achieve the highest ionic conductivities.

### 1. Introduction

All solid-state battery is one of the main targets on microelectronic integration and storage of energy. Due to the increasing interest in solid electrolytes, a large effort for understanding long-range limiting reasons for Li mobility is now under progress. At present, the study of ion motion mechanisms has many points that still deserve study in fast ion conductors [1].

In many cases, the variation of the real part of the conductivity as a function of frequency, denoted “Universal Dielectric Response” (UDR) by Jonscher, displays a static (DC) and a characteristic AC dispersive part [2]. At sufficient low temperatures, a new phenomenon, called “nearly constant Loss” (NCL), was reported by Nowick in 1981[3]. This regime was characterized by a linear or almost linear frequency dependence of the AC conductivity (i.e. constant or nearly constant dielectric loss function  $\epsilon''(\omega)$ ) and a weak temperature variation [3, 4]. At low temperatures, NCL has been observed in a broad number of liquids, glasses and crystalline solids; suggesting the existence of a universal response that has not been always recognized[5]. The NCL behaviour has also been observed in the frequency range extending from 1 mHz up to GHz.

The simultaneous presence of UDR and NCL makes the possible connection between both regimes one interesting point to be debated in solid electrolytes. Some authors believe that there does not exist any relation [6-9]; but others claim that the correlation between NCL regime and DC-conductivity is mandatory [10, 11]. In general, it has been shown that normalized ( $\sigma'(\omega)/\sigma'_{dc}$ ) vs ( $\omega/\sigma'_{dc}\cdot T$ ) plots often matches both electric UDR and NCL

responses [12]. In this analysis, some authors have found that the UDR/NCL crossover frequency is temperature dependent with activation energy lower than that of DC-conductivity[13]. In this case, the crossover activation energy has been associated with the potential energy barrier that ions have to overcome to abandon their structural sites. This conclusion suggests that NCL contribution does not go in parallel to UDR, but UDR is a consequence of NCL at increasing temperatures [14].

The Ngai's coupling model predicts slope changes when going from UDR to NCL regimes. In this context, the NCL cannot work in parallel with the UDR response. However, the series NCL contribution can only be considered as a first approach, as no analytical expressions are available to describe the evolution from NCL to hopping contribution[15]. Macdonald reported the best fittings when using parallel circuit arrangements to describe the electric response. The absence of an explicit expression for NCL to UDR behaviour makes that an “extended Jonscher expression” has often be used to describe conductivity in complex non-linear least square (CNLS) fittings.

The analysis of published papers related to NCL phenomena suggests that the strength of the NCL must be related to the network polarizability and/or mobile ions concentration, [16, 17] so that different NCL behaviours can be expected in different crystalline structures

In this paper, a parallel NMR and broad-band conductivity study has been performed on two of the best crystalline Li conductors: La<sub>0.5</sub>Li<sub>0.5</sub>TiO<sub>3</sub> perovskites and Li<sub>1.2</sub>Ti<sub>1.8</sub>Al<sub>0.2</sub>(PO<sub>4</sub>)<sub>3</sub> NASICON compounds, with rhombohedral structure (S.G R-3c)

displaying ion conductivities close to  $10^{-3} \text{ S cm}^{-1}$  at 300K. In this work, important differences have been detected in the low temperature NCL contribution of the samples, affording new insights to the NCL regime and its possible relation to the diffusion hopping processes.

## 2. Experimental section

### Samples preparation

The polycrystalline  $\text{Li}_{0.5}\text{La}_{0.5}\text{TiO}_3$  sample was prepared by solid state reaction from stoichiometric mixtures of high purity  $\text{LiOH}\cdot\text{H}_2\text{O}$ ,  $\text{La}_2\text{O}_3$  and  $\text{TiO}_2$  [18]. Possible Li losses produced during calcinations were minimized using slow heating rates ( $1^\circ/\text{min}$ ). Pellets of the reacted powder were fired at 1375 K in air for 12h; afterwards, samples were re-grounded in agate mortar, compacted again and re-fired in air at 1475 K for 12 h. From this temperature, the samples were quenched into liquid nitrogen.

The NASICON  $\text{Li}_{1.2}\text{Ti}_{1.8}\text{Al}_{0.2}(\text{PO}_4)_3$  sample was prepared by heating at 1225K stoichiometric mixtures of  $\text{Li}_2\text{CO}_3$  ( $\geq 99\%$ ),  $\text{TiO}_2$  (99%),  $\text{Al}_2\text{O}_3$  (99.99%), and  $(\text{NH}_4)_2\text{HPO}_4$  ( $\geq 99\%$ ) [19]. The reagents were first dried at 390K for 10 h and then mixed in agate mortar and heated in a platinum crucible at increasing temperatures up to 1250 K at low heating rate ( $1^\circ/\text{min}$ ).

In all cases, XRD patterns of samples were analyzed to confirm the elimination of starting reagents and the formation of final compounds. The temperature and reaction times were chosen to minimize the formation of secondary phases.

### AC impedance measurements

In fast ion conductors, the enlargement of the frequency window to higher frequencies is necessary. When the frequency window does not cover properly the range covered by UDR and NCL regimes, the correct evaluation of conductivity parameters becomes difficult [20]. To achieve the proper characterization of Li fast-ion conductors at increasing temperatures, the frequency range was extended here by using three experimental set-ups:

(i) An automatically controlled Agilent Precision LCR E4980-A Analyzer for the 20Hz-2MHz range between 77K and 550K. The sample was placed in a JANIS VPF 750 cryostat, allowing 4L-configuration measurements.

(ii) An automatically controlled Agilent E4991-A RF Impedance/Material Analyzer in the 1MHz-3GHz interval in the temperature range 150-550K. In conductivity determinations, the coaxial line was interrupted by inserting the sample between the central conductor of the Wiltron 18A50 air-line and the short. The signal was 100 mV, the number of measured frequencies 200. The result at each frequency is the average of 100 measurements. The result at each temperature is the average of three frequency sweeps

In all samples, the relative density of pellets was near 90%. To

perform the electrical characterization in the 20 Hz to 3GHz range, pellets of 3mm diameter and 0.5mm thickness were cut from larger ceramics. When the larger surfaces of the pellets were polished until mirror finishing, sputtered Pt electrodes were deposited in polished surfaces. Then, Pt Au paste electrodes were painted and sintered at 1123 K. After sintering, paste electrodes were finally polished.

(iii) Time-domain THz spectroscopy measurements were performed in the transmission mode using an amplified femtosecond laser system. Two identical 1 mm thick [110] ZnTe single crystals were used to generate and detect THz pulses. Experimental details of the custom-made setup are described elsewhere [21]. The THz technique allows the determination of the complex dielectric response,  $\epsilon^*(\omega) = \epsilon'(\omega) - i\epsilon''(\omega)$ , in the 3-80  $\text{cm}^{-1}$  range (0.1–2.4 THz). Samples for THz measurements were parallelepipeds of  $10 \times 10 \times (0.1-0.3) \text{ mm}^3$ . The major surfaces were polished to mirror finishing.

### NMR measurements

$^7\text{Li}$  ( $I = 3/2$ ) NMR spectra were recorded at room temperature in a SXP 4/100 spectrometer, after irradiation of samples with  $\pi/2$  radiofrequency pulses of 4  $\mu\text{s}$ . The frequency used for  $^7\text{Li}$  was 11 MHz. Spectra were recorded in the temperature range 100–500 K.  $^7\text{Li}$  NMR chemical shifts were referred to a 1M LiCl aqueous solution.

Quadrupole interactions detected in  $^7\text{Li}$  NMR spectra remain small ( $C_Q < 70\text{KHz}$ ), making the irradiation of central and satellite transitions non selective. NMR spectra fittings were performed with the Bruker WINFIT software package [22]. In both analyzed samples the variation of the quadrupole constants as a function of temperature was investigated.

$^7\text{Li}$  spin-lattice relaxation times ( $T_1$ ) were measured with the  $\pi$ - $\tau$ - $\pi/2$  sequence. In analyzed samples, the recovery of magnetization was exponential. Reciprocal spin-spin relaxation times ( $T_2^{-1}$ ) were deduced from the full-width at half-maximum (FWHM) of central NMR components recorded in static conditions. In the case of Gaussian lines,  $T_2^{-1}$  was calculated as  $0.6\pi$  times the FWHM central line, in the case of Lorentzian lines  $T_2^{-1}$  was calculated as  $\pi$  times the FWHM.

## 3. Results

### XRD analysis

XRD patterns of analysed samples indicate that prepared samples are single phases, maintaining their corresponding rhombohedral structure (space group R-3c in the temperature range 200-500K) [23, 24]. High temperature phase transitions detected in perovskite LLTO-05 were analyzed in previous work [25].

### AC Electric characterization.

In fast ionic conductors, conductivity relaxation times are usually short and the grain boundary contribution reduces the frequency window, limiting the detection of the bulk (i.e. grain) DC-plateau at high temperatures. This restriction is severe when analysing conductivity dispersions in fast-ion conductors.

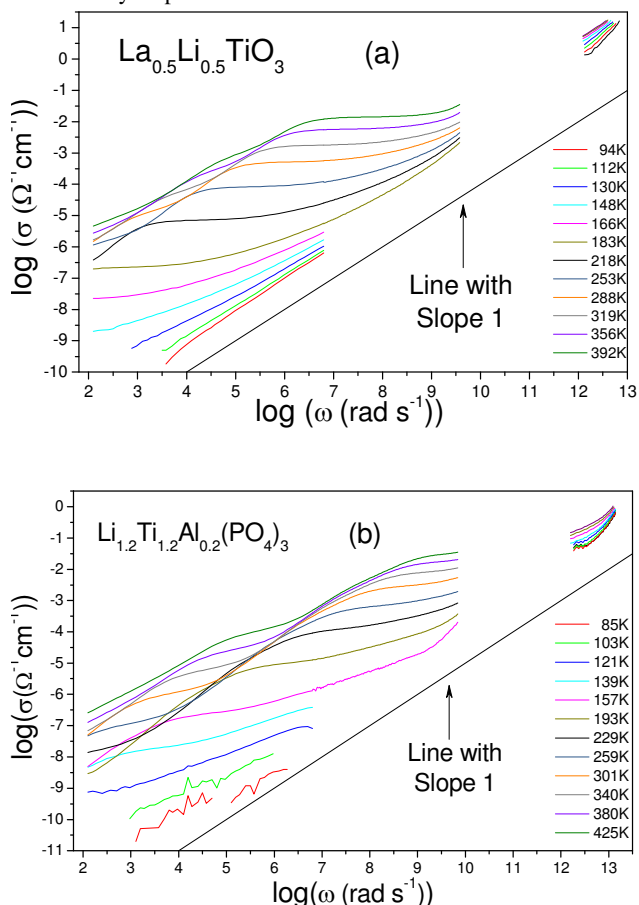


Figure 1. Frequency and Temperature dependences of the conductivity (a) LLTO-05 and (b) LTAPO-02. The measuring temperatures are depicted in the plot.

The frequency dependence of the real part of conductivity was determined by using two experimental set-ups described in the experimental section. In measured frequency and temperature ranges, grain boundary blockings, “bulk” DC-plateaus and high-frequency dispersions were studied. At 183K the typical response of ionic conductors with the transition from the UDR to NCL regimes was detected in the perovskite sample, see figure 1a. In the case of the NASICON sample the transition between both dispersive regimes is not observed, figure 1b. In both figures, THz measurements (measured between 100K and 450K), were included.

To highlight changes produced at increasing frequency, the mathematical derivative  $D_{\log \omega}(\log \sigma)$  was calculated [26]. In Figure 2a, the frequency dependence of derivative values of LLTO-05 conductivity is shown at different temperatures. In this plot, the minimum of derivative values corresponds to the bulk DC-plateau. The evolution from the DC-conductivity plateau to the UDR response (derivative value close to 0.6), and the onset of the NCL regime (derivative value near to 1) were detected between 183 and 253K. At increasing frequencies the derivative

presents values closer to one (NCL regime). At high temperatures, derivative values larger than 1 indicate the presence of undesired/spurious effects on the air-line compensation.

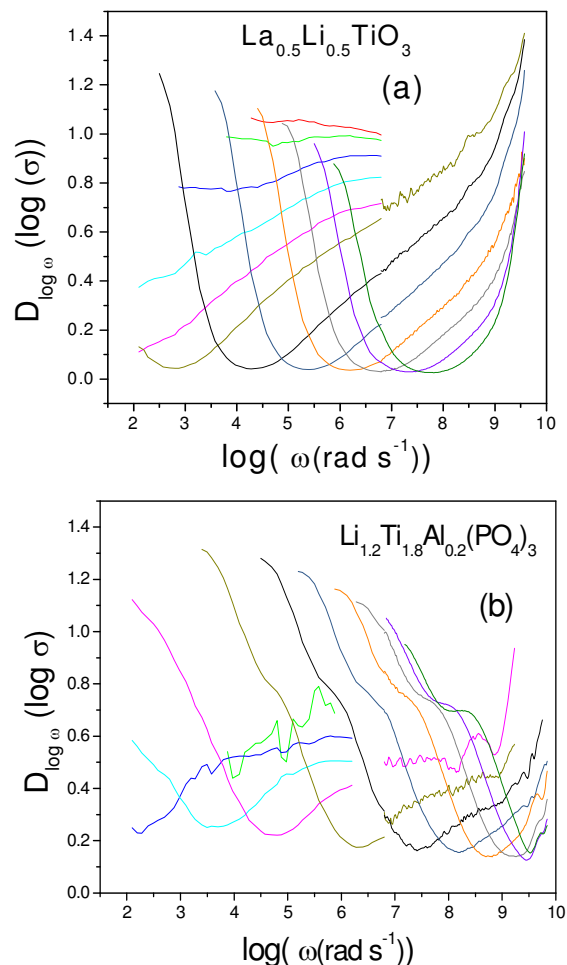


Figure 2. Plot of  $d \log \sigma / d \log \omega$  vs  $\log \omega$  (a) LLTO 05 and (b) LTAPO 02. Colors of lines correspond to those in Figure 1. The temperatures are the same as in figure 1

The conductivity response of the LTAPO-02 sample is different from that reported in LLTO-05 perovskite. In this sample the onset of the NCL behaviour was not observed in experimental plots. The electric response is mainly formed by the evolution from the bulk plateau to the UDR response. In Figure 2b, the “derivative criterion” plot is depicted. In this plot, the maximum derivative value reaches the 0.7 value, without detection of the NCL regime (slope near to 1). At higher frequencies the derivative value increases to values larger than 1, associated again to some problems with the air-line compensation.

In Figure 3, the response of two samples including the extrapolation of experimental data to THz measurements is given at 300 K. In this figure, it is clear that THz conductivity is higher for LLTO-05 than for LTAPO-02 sample, despite the larger “bulk” conductivity at RT of the latter. The extrapolated straight line joining two experimental sets of data displays slopes near 1.1 for LLTO-05 and 0.44 for LTAPO-02 samples. The results described here indicate that the UDR behaviour dominates the

high-frequency conductivity response of the NASICON sample, but the NCL response dominates that of the perovskite.

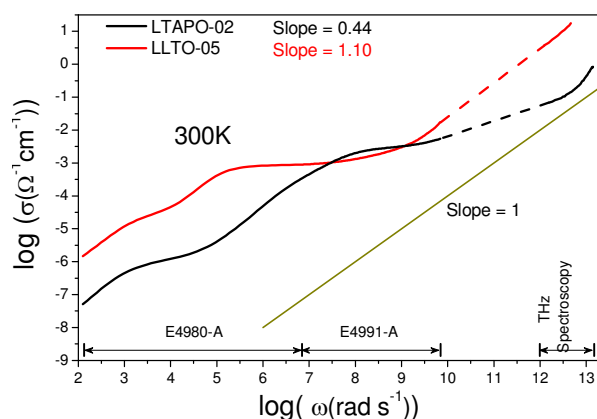


Figure 3. Frequency dependence of the conductivity at room temperature, covering about 10 decades of frequency.

The real part of the relative dielectric permittivity is qualitatively similar for the two samples, see figure 4 a,b. At high frequencies and low temperatures, a constant value for the relative permittivity is obtained. This value was detected near 114 and 14 in LLTO-05 and LTAPO-02 samples. In both samples, the THz dielectric response decreased to 90, and 10, respectively. It should be noted that the LLTO-05 sample shows a larger temperature dependence of the relative permittivity. The imaginary part of the complex permittivity corresponds to dielectric losses, figure 4 c,d. At first glance, the dielectric behaviour of the NASICON sample is different from that reported in perovskite. At the lowest temperatures, a constant value of dielectric losses was detected in perovskite that increases slightly with temperature (figure 4c).

The strength of the NCL response can be estimated with the expression:

$$A = \epsilon'' \epsilon_0 \quad (1)$$

where  $\epsilon''$  is the relative dielectric loss and  $\epsilon_0$  is the vacuum permittivity.  $\epsilon''$  values are 1.23, for LLTO-05 and 0.01 (estimated) for LTAPO-02 at the lowest measured temperatures, see figure 4 c,d. The activation energy of the NCL regime is quite low for perovskite (almost zero at low temperatures and frequencies near MHz). The NASICON samples present an activation energy for dielectric losses that is compatible with that deduced from the UDR behaviour.

In analyzed samples, two activation energies were found in the  $\sigma T$  plots of the "bulk" response (Arrhenius plots).

The perovskite LLTO-05 displays activation energy values near 0.35 eV at low temperatures, decreasing to 0.31 eV at increasing temperatures. The NASICON LTAPO-02 presents the lowest activation energy at low temperatures, 0.28 eV, decreasing to 0.24 eV at higher temperatures. At high temperatures, both samples display similar bulk DC-conductivity values.

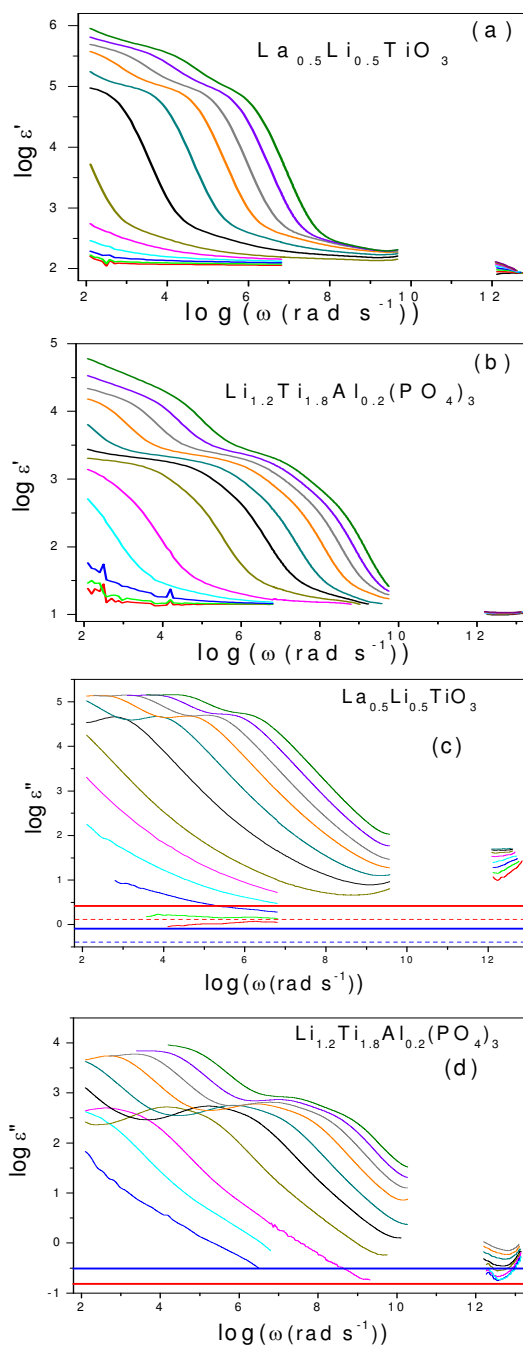


Figure 4. Frequency dependence of the relative permittivity as function of temperature. (a) Dielectric constant Real part LLTO 05 ceramic. (b) Dielectric constant LTAPO-02 ceramic. (c) Dielectric loss behaviour LLTAPO-02 ceramic. (d) Dielectric loss behaviour LTAPO-02 ceramic. The red lines are the calculated NCL at 150K using the experimental  $\epsilon'_{THz}$  values for NCL dispersion values of  $p=0.98$  solid line and  $p=0.99$  dashed line. The blue lines are the calculated NCL at 150K using the deduced  $\epsilon'D_{\infty}$  values for  $p=0.98$  solid line and  $p=0.99$  dashed line. The temperatures in all the plots are the same as in figure 1 except for the figure (d) where the 83 K and 103K are not included because of the large experimental noise.

Another interesting parameter related to the conductivity is the inverse of the dielectric relaxation time  $\omega_p$  represented in Figure

5, deduced from the conductivity plots, using the Jonscher's relation:

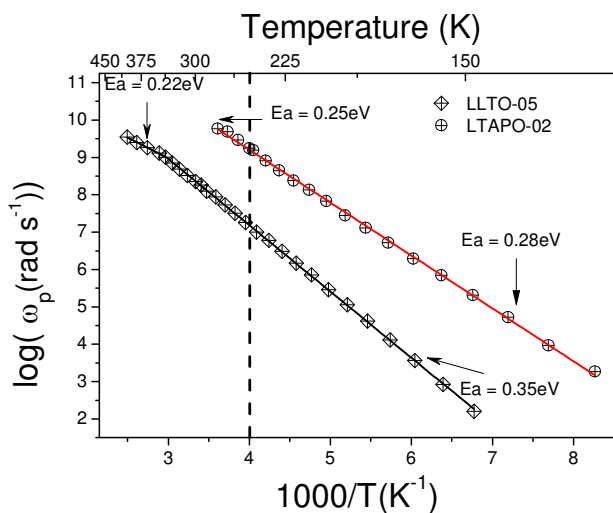


Figure 5. Temperature dependence of the attempt frequency ( $\omega_p$ ) calculated from the Real part of the complex conductivity using equation (2).

$$\sigma(\omega) = \sigma_0 \left[ 1 + \left( \frac{\omega}{\omega_p} \right)^n \right] \Rightarrow \sigma(\omega_p) = \sigma_0 \left[ 1 + \left( \frac{\omega_p}{\omega_p} \right)^n \right] \Rightarrow \sigma(\omega_p) = 2\sigma_0 \quad (2)$$

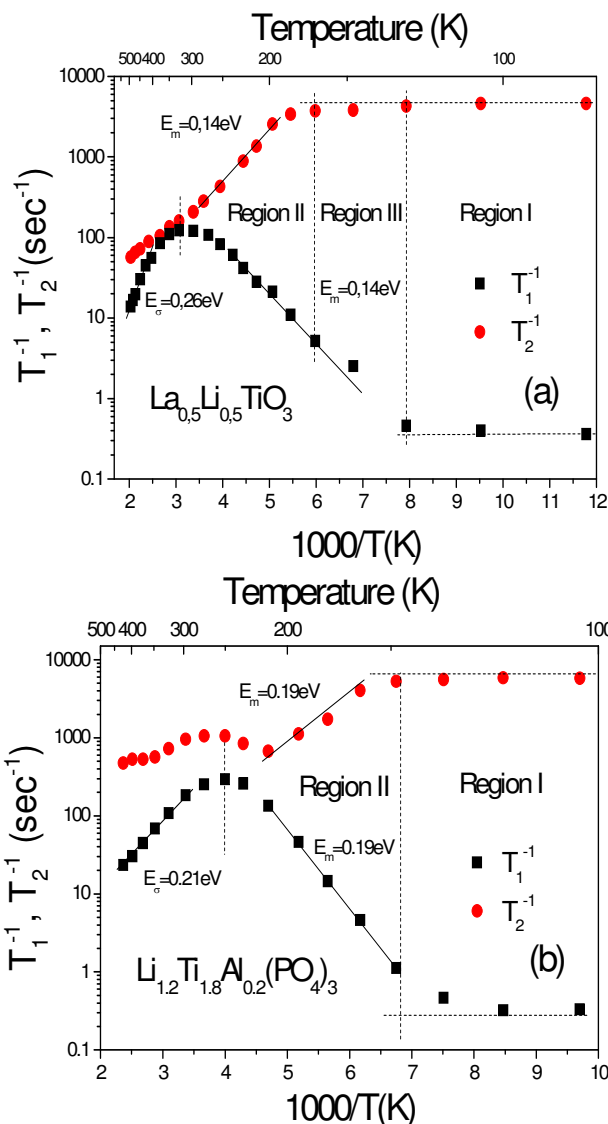
The frequency  $\omega_p$  corresponds to the attempt frequency at the measured temperature. Activation energies deduced from  $\omega_p$  agree with those deduced from the "bulk" conductivity in the same temperature range. Attempt frequencies are similar in perovskites and larger in the NASICON materials. At 250K, a difference of 2 orders of magnitude was detected between LTAPO-02 and LLTO-05.

NMR results.

$^7\text{Li}$  ( $I = 3/2$ ) NMR spectra are formed by three components that are ascribed to the central ( $-1/2 \rightarrow 1/2$ ) and satellite ( $-3/2 \rightarrow -1/2$  and  $1/2 \rightarrow 3/2$ ) transitions [18, 19]. These transitions are produced by quadrupolar interaction of Li ions with electric field gradient at occupied sites. In perovskites, the local Li motions average the quadrupole interactions making difficult the detection of residual interactions; however, in the Nasicon sample, three transitions are visible.

In Figure 6, the temperature dependence of  $^7\text{Li}$  NMR spin-lattice ( $1/T_1$ ) and spin-spin ( $1/T_2$ ) relaxation rates of LLTO-05 and LTAPO-02 samples are plotted in the temperature range 100-500K. Dipolar interactions of Li with atoms disposed at short distances produce the broadening of the central transition (proportional to  $1/T_2$ ). Li mobility decreases  $1/T_2$  and increases  $1/T_1$  relaxation rates. At increasing temperatures,  $1/T_1$  values

pass through a maximum near 300 and 250K in LLTO-05 and LTAPO-02 respectively. At the maxima, residence times of Li ions at structural sites verify the relation  $\tau_R \approx 1/\omega_0 \approx 10^{-8}$  s.



In LLTO-05, spin-spin relaxation rates  $T_2^{-1}$  remains constant in the temperature range 100-190K, region I in figure 6 a, indicating  $^7\text{Li}$  NMR spin-lattice ( $1/T_1$ ) and spin-spin ( $1/T_2$ ) relaxation rates of the (a) LLTO-05, and (b) LTAPO-02 samples.

the absence of Li mobility. The spin-lattice relaxation rates  $T_1^{-1}$  display different slopes at both sides of the maximum. In the temperature range 170-250K, activation energy is 0.14 eV; but in the range 350-500 K the activation energy is 0.26 eV. The temperature at which  $T_2^{-1}$  decreases, is considerably higher that corresponding to the  $1/T_1$  increment, region III in figure 6 a. This observation has been ascribed to the existence of local motions that does not change the mean Li-Li distances (dipolar interactions), but produces an efficient spin-lattice relaxation. Above 160 K, hopping motions are responsible for the  $1/T_1$  increment and  $1/T_2$  decrement, region II in figure 6 a.

The temperature dependence of NMR relaxation rates in LTAPO-02 differs from that detected in LLTO-05 perovskites. In particular, the  $T_1^{-1}$  maximum is symmetric in the first case, but clearly asymmetric in the second one. At the low temperature branch, the activation energy is 0.19 eV but at the high temperature branch, the activation energy is 0.21 eV. The spin-spin relaxation rate  $1/T_2$  is constant in the interval 100-170 K, indicating that Li mobility increases appreciably only above 160K, region I in figure 6b. This temperature matches with the increment detected in the spin-lattice relaxation plot, indicating that long range motions are directly established in LTAP-02 sample, region II in figure 6b. The temperature dependence of  $1/T_2$  plots is complex indicates the presence of two relaxation mechanisms in the LTAP-02 sample. These two relaxation mechanisms could not be resolved in  $1/T_1$  plot of the Nasicon system.

#### 4. Discussion

The electric behaviour of perovskite and NASICON samples differs considerably at low temperatures. In the case of the NASICON system, the NCL regime is negligible or absent but in the case of perovskites this contribution is important. As electric measurements have been measured with the same blocking electrodes, we can conclude that the NCL contribution cannot be ascribed to the series electrode polarization often invoked in previous papers.

In literature, the NCL contribution has been related to ion oscillations in potential well-cages that slowly decay with

time[27]. In this approximation, a thermally activated cross-over from NCL to UDR process should be observed in conductivity plots. This approximation forced a series link between NCL and UDR regimes that implies that NCL has to be cancelled when hopping behaviour starts. In this case, all ions that are participating to hopping behaviour, leading to the dc-conductivity, should have been involved in NCL processes. A relationship between the magnitude of the constant loss value (A) and the DC-conductivity was proposed by Leon et al. for a large variety of ionic conductors [28]. These authors suggest that:

$$A \propto \frac{1}{E_a} [1 - (T/T_0)]^{-1} \quad (3)$$

where  $E_a$  is the microscopic activation energy and  $T_0$  is the temperature related to the onset of the NCL behaviour. Using this expression they found a good correlation between  $E_a$  and A in a wide variety of solid electrolytes. In Figure 6 we have plotted the curve obtained by Leon et al. (Figure 1 of Ref 28) including our results for LLTO-05 and LTAPO-02 samples. In the case of

perovskites our results agree with published results; however, in the case of the NASICON, our results are lower those reported in other samples and far below the model curve.

In previous works, Macdonald concluded that local ion motions, related to the NCL contribution, must be related to the bulk polarization [17]. On the other hand, Nowick et al. [29] ascribed the NCL to off-centering local motions of atoms. In relaxor ferroelectrics, which are high-permittivity disordered dielectrics, the NCL regime observed at low temperatures was assigned to hopping of polar nanoregions over a broad distribution of potential barrier heights [30].

The concentration of mobile ion has also a significant influence on the shape and strength of the NCL. In diluted systems (low carrier concentration), instead of the constant loss regime a Debye-like peak was found that smeared out on increasing the carrier concentration [29]. Based on previous studies, both mobile ion concentration and "bulk" polarizability must contribute to the NCL response. Taking into account that NCL is related to dipolar moments and that they enhance the dielectric constant at high frequency, it is important to understand its influence at microscopic level.

In a recent paper, Macdonald [17] proposed that the high frequency dielectric constant is formed by two contributions

$$\epsilon'_{\infty} = \epsilon' C_{\infty} + \epsilon' D_{\infty} \quad (4)$$

where  $\epsilon' C_{\infty}$  is related to the ion motion and  $\epsilon' D_{\infty}$  to the "bulk" polarization of the structure. In the case of the  $\epsilon' C_{\infty}$  the relationship with charge carriers concentration is

$$\epsilon' C_{\infty} = \frac{\gamma N (qd)^2}{6kT\epsilon_0} \quad (5)$$

where  $N$  is the concentration of charge carriers,  $\gamma$  the fraction of mobile ions,  $(qd)$  the induced dipolar moment and other parameters have the usual meaning. The high-frequency dielectric constant is then related to ionic conductivity is proportional to the number of charge carriers, their charge  $q$  and their displacement  $d$ .

Then  $\epsilon' C_{\infty}$  can be compared with the expression of DC conductivity, [29]

$$\sigma(0) = \frac{(qd)^2 c_0 \omega_{AV}}{6kTV_m} \quad (6)$$

where  $c_0$  is the concentration of mobile ions,  $V_m$  is the molar volume,  $\omega_{AV}$  is the mean jump frequency and other symbols have their usual meaning.  $\omega_{AV}$  is the result of multiply the probability to move by the jump attempt frequency of free carriers ( $\omega_p$ ), see

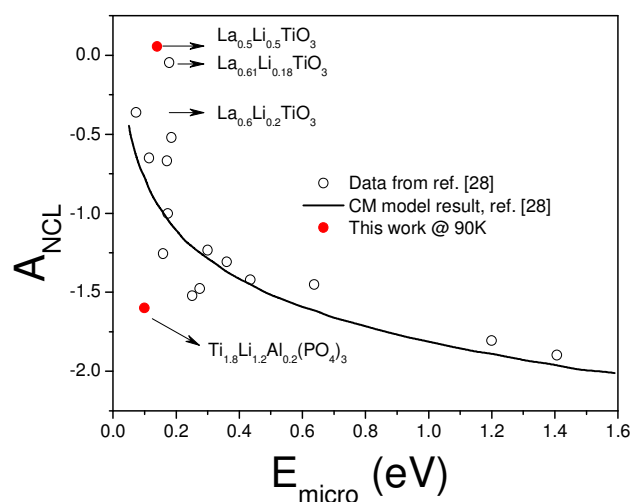


Figure 7. Relationship between the NCL strength  $A$  and the microscopic activation energy  $E_m$  deduced from NCL and UDR regimes (from ref. [28]). In this plot values deduced in this work (solid circles) are included.

equation 2. Nowick et al[29] demonstrated that  $\omega_{AV} \approx \omega_p$  (exactly speaking  $\omega_{AV} \leq \omega_p$ ), because probability lies between 0 and 1.

The DC conductivity can be also expressed as:

$$\sigma(0) = K_n \omega_p \quad (7)$$

where

$$K_n = (qd)^2 c_0 / 6kTV_m \quad (8)$$

The DC conductivity can be related to the equation 5 for  $\epsilon' C_\infty$ , because  $\gamma N$  can be expressed as  $c_0/V_m$  and so

$$\epsilon' C_\infty = K_n / \epsilon_0 \quad (9)$$

The value of  $K_n$  at each temperature can be deduced from experimental AC conductivity values using equations 2 and 7. If the calculation is made at 150K,  $\log K_n$  of LLTO-05 and LATPO 02 samples display -11.16 and -12.38 values respectively. Applying equation 9 to calculate  $\epsilon' C_\infty$  values of 78 and 5 were obtained respectively.

On the other hand,  $\epsilon'$  values can be estimated at 1MHz at the same temperature. If calculated  $\epsilon' C_\infty$  values are subtracted from the relative dielectric permittivity values at 1 MHz and 150 K (134, and 15),  $\epsilon' D_\infty$  values of 56 and 10 were deduced. If these values are compared with the relative dielectric constant measured in the THz range ( $\epsilon'_{THz}$ ) at the same temperature, 98 and 10 values were obtained, see figures 4 a,b. At this very high frequency the contribution to the permittivity of the mobile ions must be small. It is interesting to note the close agreement between calculated  $\epsilon' D_\infty$  and observed  $\epsilon'_{THz}$  values for the

NASICON samples, indicating that permittivity is related to pure “bulk” effect and so at 1MHz the dielectric constant is the sum of the structure polarizability and the contribution of the moving ions. However, calculated  $\epsilon' D_\infty$  values are much lower than  $\epsilon'_{THz}$  values in perovskites. This discrepancy should be related to the influence of the charge carriers to the THz permittivity, so in some extent moving ions are still contributing to the permittivity value in the THz region, confirming the existence of a strong coupling between  $\epsilon' D_\infty$  and  $\epsilon' C_\infty$  values in perovskites. This coupling was invoked by Macdonald to explain the relation between NCL and ionic conductivity.

Taking into account that the dispersion exponent of NCL approaches to 1, the constant phase element (CPE) formalism leads to

$$\epsilon_{NCL}^*(\omega) = B(\omega^{1-p}) \quad (10)$$

where  $B$  is very close to the real part of the relative permittivity in the frequency region where the NCL behaviour dominates. The strength of the NCL ( $A$ ) is given for  $p$  values close to 1 by

$$A \cong B \tan \delta_p \quad (11)$$

The value of  $A$  depends on  $B$  and  $p$  through the parameter  $\tan \delta_p$  (loss tangent). In Figures 4 c,d, the NCL strength calculated for  $p=0.99$  (blue) and  $p=0.98$  (red) at 150 K is included in the loss curves of LLTO-05 and LATPO-02 samples for calculated  $\epsilon' D_\infty$  values (dashed lines) and different values of high-frequency relative permittivity  $\epsilon'_{THz}$  (solid lines). The results obtained for perovskites indicate that experimental NCL values are in good agreement with those calculated by using  $\epsilon'_{THz}$  and an exponent 0.99 for NCL dispersion. In perovskite,  $\epsilon' D_\infty$  values produce small NCL values in comparison with experimental values. The result obtained for LATPO-02 indicates that the experimental NCL behaviour lies below the calculated NCL value for both possibilities and it is below the sensitivity of the experimental set-up. This result indicates a much lower coupling between ionic conductivity and THz permittivity.

The NCL effect seems to be related to the concentration of charge carriers and induced dipolar moments. The concentration of charge carriers is maximum in LLTO 05, so the NCL strength is higher. In the NASICON sample, Li dc-conductivity is one of the highest reported but NCL contribution is too small to be experimentally measured using our experimental set up. In NASICON compound the value of  $K_n$  is much lower than that of the perovskite. The low values of  $K_n$  parameter and polarizability of the NASICON structure can be the responsible for the low value of  $\epsilon'_{THz}$  and the absence of a measurable NCL response. The high ionic conductivity detected in the NASICON samples must be related to a higher ionic mobility of Li, as indicated by high  $\omega_p$  values measured. At present, the remaining question is the origin of low  $K_n$  values in the NASICON sample. Despite both structures presents the same space group of symmetry, the topology and the structural positions occupied by the Li ions is different. In LLTO-05, Li ions and vacancies are randomly distributed in A sites of the perovskite [25], however, in LATPO-02 Li ions are preferentially located at M1 sites and most

vacancies are disposed near M2 interstitial sites [19]. The different distribution of Li ions and vacancies in both structures must lead to different conductivity mechanism.

5 The influence of the pre-movements leading to NCL behaviour in perovskite and NASICON samples is reflected in the NMR response. For the perovskite three regions of behaviour are clearly observed in the perovskite and only two in the NASICON sample. The region III is related to the existence of local motions  
10 that does not change the mean Li-Li distances (dipolar interactions) and so do not change the spin-spin relaxation ( $1/T_2$ ), but produces an efficient spin-lattice relaxation ( $1/T_1$ ). This region III is almost suppressed in the NASICON sample. This difference supports the idea of the absence of important local  
15 motions in the NASICON sample responsible of large NCL responses.

At present, two scenarios can be imagined. In the first one, it can be assumed that NCL response is not present in NASICON  
20 samples, and ions go directly from a stationary position to the hopping process. This should be related to atom oscillations around lattice positions, that do not generate dipolar moments. The absence of NCL response does not prevent, however, the existence of other structural sources that produce similar  
25 polarizations. The second scenario is that NCL is not absent but is very small. Returning to the model equation (3), this means that the proportionality constant is much lower than observed in perovskites. In the case of the NASICON, the NCL regime should be very small even at the lowest temperatures, indicating  
30 that vibration of ions in potential well-cages does not induce strong relaxations, remaining vibrations similar to those predicted by Debye approximation.

From our results it is difficult to find an explanation for  
35 differences on the NCL behaviour of perovskite and NASICON compounds. As it has been pointed out by some authors [17], the polarization of the structure plays an important role in the NCL response. The study of the terahertz permittivity at low temperatures has shown a larger value for LLTO-05 (90) than  
40 LATPO-02 (10). This analysis proves that perovskites are much more polarisable than NASICON samples. In other words, the phonon contributions to static permittivity must be much higher in LLTO-05 than in LATPO-02.

45 The dielectric behaviour of the  $\text{La}_{0.53}\text{Na}_{0.41-x}\text{Li}_x\text{TiO}_3$  perovskites was studied by Katsumata et al. [31] for samples with  $x < 0.12$ , they found a quantum paraelectric behaviour and for  $x = 0.08$  and  $0.012$  a broad ferroic dielectric peak. Both are signatures of a highly polarisable network. In  $\text{La}_{0.5}\text{Na}_{0.5}\text{TiO}_3$  the permittivity is  
50 more than 100 and increases on cooling due to the polar phonon softening [32]

From this analysis, it can be concluded that the presence of strong NCL is not required for achieving high values of ionic  
55 conductivity. This conclusion can be derived from the study of the NASICON sample, where NCL contributions could not be detected. To confirm this idea, additional work must be done to find structural reasons that explain high conductivity values

measured in NASICON compounds with a such low  $K_n$  value.

## 60 5 Conclusions

A parallel NMR and Impedance Spectroscopy study of  $\text{La}_{0.5}\text{Li}_{0.5}\text{TiO}_3$  (LLTO-05) perovskite and  $\text{Li}_{1.2}\text{Ti}_{1.8}\text{Al}_{0.2}(\text{PO}_4)_3$  (LATPO-02) NASICON compounds by spectroscopy has been performed in the temperature range 100-500K. In both cases, a  
65 three dimensional conduction network is present in rhombohedral (R-3c S.G.) phases, In LLTO-05, Li ions and vacancies are randomly distributed in A sites of the perovskite, however, in LATPO-02 Li ions are preferentially located at M1 sites and most vacancies are disposed near M2 sites.

70 In two types of compounds, correlated UDR motions are detected between 250 and 500 K, however, local motions at lower temperatures are different. In perovskite, local motions produced inside unit cells are responsible for the NCL regime; however, in  
75 the NASICON phase, local motions not participating to the long range regime, were almost absent. In both types of samples, long-range motions are responsible for e bulk DC-conductivity values near  $10^{-3} \text{ S.cm}^{-1}$  at R.T., indicating that a strong NCL contribution at high-frequency and low-temperature, related to the local  
80 motions of the charge carriers, is not required to achieve important ionic conductivity values.

## AUTHOR INFORMATION

### Corresponding Author

85 \*Ricardo Jiménez.

Email: riqjim@icmm.csic.es

### Notes and references

<sup>a</sup> Instituto de Ciencia de Materiales, ICMM-CSIC C/ Sor Juana Inés de la Cruz 3, 28049 Cantoblanco, Madrid – Spain.

90 <sup>b</sup> Institute of Physics, Academy of Sciences of the Czech Republic, Na Slovance 2, 182 21 Prague 8, Czech Republic.

<sup>c</sup> Departamento de Ciencia de Materiales, Universidad Carlos III de Madrid Avenida Universidad 30, 28911 Leganés-Spain.

## ACKNOWLEDGMENTS

100 Authors thank MINECO (project MAT2010-19837-C06-02) and the regional Government (project S-2009/PPQ 1626) for financial support. S.K and D.N. were supported by Czech Science Foundation (Project No. P204/12/02321163). We would like to  
105 thank Prof. J.R Macdonald for stimulating discussions..

## References

[1] J.C. Dyre, P. Maass, B. Roling, D.L. Sidebottom, Reports on Progress  
110 in Physics 72 (2009) 046501

- [2] A.K. Jonscher, *Journal of Physics D: Applied Physics* 32 (1999) 57-70
- [3] W.K. Lee, J.F. Liu, A.S. Nowick, *Physical Review Letters* 67 (1991) 1559-1561
- 5 [4] A. Rivera, J. Santamaría, C. León, J. Sanz, C.P. Varsamis, G.D. Chryssikos, K.L. Ngai, *Journal of Non-Crystalline Solids* 307-310 (2002) 1024-1030
- [5] J.R. Macdonald, *Journal of Applied Physics* 75 (1994) 1059-1069
- [6] B. Roling, C. Martiny, S. Murugavel, *Physical Review Letters* 87  
10 (2001) 085901
- [7] D.L. Sidebottom, C.M. Murray, *Physical Review Letters* 89 (2002) 195901
- [8] S. Murugavel, B. Roling, *Journal of Non-Crystalline Solids* 330 (2003) 122-127
- 15 [9] D.L. Sidebottom, *Physical Review B* 13 (2005) 134206
- [10] C. León, A. Rivera, A. Várez, J. Sanz, J. Santamaria, C.T. Moynihan, K.L. Ngai, *Journal of Non-Crystalline Solids* 305 (2002) 88-95
- [11] C. León, K.L. Ngai, A. Rivera, *Physical Review B* 69 (2004) 134303
- [12] B. Roling, A. Happe, K. Funke, M.D. Ingram, *Physical Review Letters* 78 (1997) 2160-2163
- 20 [13] C. León, A. Rivera, A. Várez, J. Sanz, J. Santamaria, *Physical Review Letters* 86 (2001) 1279-1282
- [14] K.L. Ngai, R. Casalini, *Physical Review B* 66 (2002) 132205
- [15] J.R. Macdonald, *Journal of Applied Physics* 94 (2003) 558-565
- 25 [16] J.R. Macdonald, *Physical Review B* 66 (2002) 064305
- [17] J.R. Macdonald, *Journal of Chemical Physics* 116 (2002) 3401-3409
- [18] J. Ibarra, A. Várez, C. León, J. Santamaría, L.M. Torres-Martínez, J. Sanz, *Solid State Ionics* 134 (2000) 219-228
- [19] K. Arbi, S. Mandal, J.M. Rojo, J. Sanz, *Chemistry of Materials* 14  
30 (2002) 1091-1097
- [20] H. Jain, C.H. Hsieh, *Journal of Non-Crystalline Solids* 172-174 (1994) 1408-1412
- [21] P. Kužel, J. Petzelt, *Ferroelectrics* 239 (2000) 949-956
- [22] D. Massiot, WINFIT, Bruker-Franzen Analytik GmbH, Bremen,  
35 Germany, 1993
- [23] K. Arbi, M. Tabellout, M.G. Lazarraga, J.M. Rojo, J. Sanz, *Physical Review B* 72 (2005) 094302
- [24] J. Ibarra, A. Várez, C. León, J. Santamaria, L.M. Torres, J. Sanz, *Solid State Ionics* 134 (2000) 219-228
- 40 [25] A. Várez, Y. Inaguma, M.T. Fernández, J. Alonso, J. Sanz, *Chemistry of Materials* 15 (2003) 4637-4641
- [26] W. Bucheli, R. Jimenez, J. Sanz, A. Várez, *Solid State Ionics* 227 (2012) 113-118
- [27] A. Rivera, C. León, C.P. Varsamis, G.D. Chryssikos, K.L. Ngai,  
45 C.M. Roland, L.J. Buckley, *Physical Review Letters* 88 (2002) 125902
- [28] C. León, K.L. Ngai, A. Rivera, *Physical Review B* 69 (2004) 134303
- [29] A.S. Nowick, B.S. Lim, *Physical Review B* 63 (2001) 184115
- [30] I. Rychetsky, S. Kamba, V. Porokhonsky, A. Pashkin, M. Savinov,  
50 V. Bovtun, J. Petzelt, M. Kosec and M Dressel. *J. Phys.: Condens. Matter* 15 (2003) 6017-6030
- [31] T. Katsumata, Y. Inaguma, *Solid State Ionics* 154-155 (2002) 795-799
- [32] F. Borodavka, E. Simon, I. Gregora, S. Kamba, R. Haumont and J.  
55 Hlinka, *J. Phys.: Condens. Matter* 25 (2013) 085901M. Mehring, *Coord. Chem. Rev.*, 2007, **251**, 974

60

65

70